King Saud University

Arabian Journal of Chemistry

www.ksu.edu.sa
www.sciencedirect.com

SPECIAL ISSUE: ENVIRONMENTAL CHEMISTRY

Bengal Gram Seed Husk as an adsorbent for the removal of dye from aqueous solutions – Batch studies

M.C. Somasekhara Reddy *, V. Nirmala, C. Ashwini

Department of Basic Sciences, G.P.R. Engg. College (Autonomous), Kurnool 518007, AP, India

Abstract   The feasibility of using Indian Seed Husk of Bengal Gram (Scientific Name: *Cicer arietinum*) (SHBG), abundantly available in and around the Kurnool in Andhra Pradesh, for the anionic dye (Congo red, CR) adsorption from aqueous solution, has been investigated as a low cost and an eco-friendly adsorbent. Adsorption studies were conducted on a batch process, to study the effects of contact time, initial concentration of CR, de-sorption and pH. Maximum colour removal was observed at lower pH. The dye attained equilibrium approximately at 1, 1.5, 2 and 2.5 h for dye concentrations 25, 50, 75 and 100 mg/l respectively. The present dye removal decreased from 89% to 74% as the dye concentration has been increased from 25 mg/l to 100 mg/l. A maximum removal of 92% is obtained at lower pH. Adsorption decreases with increase in pH. Maximum de-sorption of 26.4% is achieved in water medium at pH 11.95. The equilibrium data were analyzed by the Langmuir and Freundlich isotherms. The data fitted well with the Langmuir model, with a maximum adsorption capacity of 41.66 mg g^{-1}. The pseudo-second-order kinetics was the best for the adsorption of CR, by SHBG with good correlation. The results suggest that SHBG is a potential low-cost adsorbent for the CR dye removal from synthetic dye wastewater.

© 2014 Production and hosting by Elsevier B.V. on behalf of King Saud University.

1. Introduction

Dyes and dye intermediates are produced in large quantities in India to meet the requirement of the world at large. Lot of fresh water is used in the dye industry and during the process the fresh water is contaminated and it is discharged as wastewater which contains lot of pollutants like dyes etc. The complex aromatic molecular structures of dyes make them more stable and more difficult to biodegrade (Wang and Li, 2007) Therefore, dye industry contributes to water pollution by discharging large volume of coloured and toxic effluent. These coloured water and wastewater are dumped into different water bodies and spoil the aquatic life and aesthetic value of the receiving water bodies (Hameed, 2009).Thus effluents from dye industries have been of major concern of water pollution in India. Dye effluents contain heavy load of pollutants like colour, pigments, tan, high total suspended salts(TSS), total dissolved solids (TDS), biological oxygen demand (BOD), chemical oxygen demand (COD) and some of them are

* Corresponding author. Mobile: +91 94410 34599.
  E-mail addresses: som16@rediffmail.com, mcsr.gprec@gmail.com (M.C. Somasekhara Reddy).
Peer review under responsibility of King Saud University.

carcinogenic and mutagenic (de Lima et al., 2007; Tsuboy et al., 2007; Carita and Marin-Morales, 2008).

The colour is the most obvious indicator of water pollution. This interferes with transmission of sunlight into streams and therefore reduces the photosynthetic activity. Considerable research has been done on colour removal from these coloured waste waters. Various techniques, such as sedimentation (Cheremisinoff, 2002), biological treatments (Kapdan and Ozturk, 2005) electrochemical coagulation and flocculation (Hai et al., 2007; Raghavacharya, 1997; Phalakornkule et al., 2010), ozonation (Slokar and Le Marechal, 1997), ion-exchange (Wu et al., 2008), membrane technology (Kim et al., 2007), sonochemical degradation (Abbasi and Asl, 2008), photochemical degradation (Gupta et al., 2007a; Sohrabi and Ghavami, 2008), electrochemical removal (Gupta et al., 2007b), electrochemical degradation (Fan et al., 2008), chemical oxidation (Neamtu et al., 2004) and adsorption (Somasekhara Reddy et al., 2012) have been generally employed for colour removal. However, of these, it has been found that adsorption technique is the most prominent for removal of dyes from wastewater (Gupta and Suhas, 2009; Pavan et al., 2008).

The activated carbon was used as adsorbent for colour removal by adsorption (Calvete et al., 2010; Lorenc-Grabowska and Gryglewicz, 2007). Due to high cost of activated carbon, lot of alternative adsorbents are developed and used for removal of colour from the aqueous solutions. A number of non-conventional, low-cost agricultural materials are used as adsorbents for removal of pollutants from wastewater. Some of them are jujube seed powder (Somasekhara Reddy et al., 2012), lentil straw (Celekli et al., 2012), tamarind fruit shell (Somasekhara Reddy, 2006), curcumas sativa Fruit peel (Santhi and Manonmani, 2011), citrus waste (Asgher and Bhatti, 2012), macuaba palm cake (Vieira et al., 2012), tannery solid waste (Piccin et al., 2012), babassu coconut epicarp (Vieira et al., 2011), cattail root (Hu et al., 2010), jute stick powder (Panda et al., 2009), peanut hull (Gong et al., 2005; Tanyildizi, 2011), soya meal hull (Arami et al., 2006), papaya seed (Hameed, 2010), spent brewery grains (Jaikumar et al., 2009), maize cob (Sonawane and Shrivastava, 2009), straw (Zhang et al., 2012), coir pith (Namasivayam et al., 1996; Khan et al., 2011), sesame hull (Feng et al., 2011), jackfruit peel (Hameed, 2009), hazelnut shells (Dogan et al., 2008), de-oiled soya (Gupta et al., 2009), hen feathers (Gupta et al., 2006), guava (Psidium guajava) leaf powder (Ponnusami et al., 2008), pumpkin seed hull (Hameed and El-Khaiary, 2008a), broad bean peels (Hameed and El-Khaiary, 2008b), castor seed shell (Oladoja et al., 2008), eggshell waste (Tsai et al., 2008), braziliun-pine fruit shell (Calvete et al., 2010), etc. But the adsorption capacities of most of the above adsorbents are limited. New, economical, locally available and highly effective adsorbents are still in the process of development.

Number of reviews are available in the literature on the utilization of agricultural wastes/by-products in the treatment of water and wastewater (Bhatnagar and Sillanppa, 2010; Crini, 2006; Somasekhara Reddy, 2005; Demirbas, 2009).

Recently tamarind fruit shell (Somasekhara Reddy, 2006) and Jujube seed powder (Somasekhara Reddy et al., 2012) are used as adsorbents for the removal of CR from the aqueous solutions and interest led us to use another agricultural solid waste, SHBG material for the removal of the same direct dye, CR from synthetic wastewater.

The aim of the present work is to find out the adsorption capacity of solid waste, SHBG, an agricultural waste for the removal of direct dye, CR from synthetic wastewater.

1.1. Theory of adsorption kinetics and isotherms

1.1.1. Kinetic models

The Lagergren's pseudo-first-order model (Eq. (1)) and Ho's pseudo-second-order model (Eq. (2)) (Somasekhara Reddy et al., 2012) have been widely used to predict adsorption kinetics. The pseudo-first-order equation is generally applicable to predict the initial stage of the adsorption process whereas the pseudo-second-order equation predicts the behaviour over the whole range of adsorption. These two models were used to fit the experimental data of this study.

$$\log(q_e - q_t) = \log q_e - (k_1/2.303)t \tag{1}$$

$$t/q_t = (1/k_2 q_e^2) + (1/q_e)t \tag{2}$$

where k_1 (min^{-1}) is the rate constant of pseudo-first-order adsorption and k_2 (g mg^{-1} min^{-1}) is the rate constant of pseudo-second-order adsorption. q_e is the amount of dye adsorbed on adsorbent at equilibrium.

1.1.2. Intra-particle diffusion model

In order to investigate the mechanism of the CR adsorption onto SHBG, intra-particle diffusion based mechanism is studied. The most commonly used technique for identifying the mechanism involved in the adsorption process is, fitting an intra-particle diffusion plot. It is an empirically found functional relationship, common to the most adsorption processes, where uptake varies almost proportionally with $t^{0.5}$ rather than with the contact time t. According to the theory proposed by Weber and Morris (Hameed, 2009).

$$q_t = k_{pi} t^{0.5} + C_i \tag{3}$$

where k_{pi} (mg g^{-1} min$^{-0.5}$), the rate parameter of stage i, is obtained from the slope of the straight line of q_t versus $t^{0.5}$ where as C_i is the intercept of the plot that gives an idea about the thickness of the boundary layer.

1.1.3. Isotherm models

Langmuir isotherm model was applied to describe the adsorption of CR. The model is represented by the following equation.

$$C_e/q_e = 1/Q_{\max}K_L + C_e/Q_{\max} \tag{4}$$

where C_e is the equilibrium concentration of CR in solution (mg L^{-1}), $Q_{\max}$ is the maximum adsorption capacity of SHBG (mg g^{-1}) and K_L is the Langmuir constant related to the adsorption energy (L mg^{-1}). R_L, a dimensionless constant, is used to determine whether an adsorption is favourable or not and is calculated by

$$R_L = 1/(1 + K_L C_0) \tag{5}$$

where C_0 is the initial concentration of CR in solution (mg L^{-1}).

Freundlich isotherm model is also applied to describe the adsorption of CR. Linearized in logarithmic form of Freundlich isotherm model equation is represented by.

$$\log q_e = \log K_F + (1/n) \log C_e \qquad (6)$$

where K_F is the Freundlich constant and '$1/n$' is the heterogeneity factor.

2. Materials and methods

2.1. Preparation of adsorbent, SHBG

The seed husk of Bengal gram (SHBG) is discarded as a waste in a small-scale industry where dal of Bengal gram (which is used in the preparation of certain food items) is separated from seed of Bengal gram. This waste is used in certain areas as foodstuff for the animals in addition to use as fire wood in hotels and restaurants. The SHBG has been collected from a local industry, which is in the nearby town, Nandyal and washed thoroughly with de-ionized water for removing dirt. The dried husk material has been ground and sieved to a desired mesh size between 53 to 75 μm. It has been abbreviated as SHBG. It has been used as an adsorbent for the removal of a direct dye, CR.

2.2. Adsorbate

Congo red (Direct red 28) (C.I.22120) (CR) was supplied free of cost by M/S Sipka Sales Corporation, New Delhi (dye supplier and manufacturer and the purity of dye is 75%) and this dye has been used without any further purification. FW = 696.7 and $\lambda_{\max}$ = 497 nm. The chemical structure is as shown in Fig. 1.

Stock solution of 1000 mg L^{-1} was prepared by dissolving accurate quantity of the dye in double distilled water. The experimental solution was obtained by diluting the stock solution to the designed Figs. 8 and 9 initial dye concentration.

2.3. Point of zero charge (pH$_{PZC}$)

The zero surface charge characteristics of SHBG were determined, using the solid addition method (Hameed, 2010; Ponnusami et al., 2008; Somasekhara Reddy et al., 2012). 40 mL of 0.1 M KNO$_3$ solution was transferred to a series of 100 mL Stopperd conical flasks. The pH$_i$ (initial pH of dye solutions i.e., pH of dye solutions before experiment) values of the solutions were roughly adjusted between 2 and 12 by adding either 0.1 N HCl or NaOH and were measured by using pH metre (Systronics pH system 361 Model, India). The total volume of the solution in each flask was exactly adjusted to 25 mL by adding KNO$_3$ solution of the same strength. The pH$_i$ of the solutions was then accurately noted. 50 mg of SHBG

Figure 1   Structure of Congo red (CR).

was added to each flask, and the flask was securely capped immediately. The suspensions were then kept shaking for 24 h and allowed to equilibrate for 0.5 h. The final pH values of the supernatant liquid were noted. The difference between the initial pH (pH$_i$) and final pH (pH$_f$) values (ΔpH) was plotted against the pH$_i$. The point of intersection of the resulting curve with abscissa, shown in Fig. 11 at pH 0, gave the pH$_{PZC}$.

2.4. Batch kinetics studies

Adsorption experiments were carried out by agitating 100 mg of adsorbent (SHBG) with 25 ml of dye solutions of desired concentration and pH in a 50 ml screw type Erlenmeyer flask at room temperature (30 ± 1 °C). A good contact was made between the adsorbent and dye by agitating at 160 rpm in a Julabo shaking water bath. Dye concentration was determined spectrophotometrically by monitoring the absorbance at 497 nm using Chemito UV–VIS Spectrophotometer and two 1-cm cells. The wavelength of the maximum absorbance for dye was selected, and $\lambda_{\max}$ value was 497 nm. The pH of dye solutions was determined using pH metre (model Li-120, Elico, Hyderabad, India). The samples were withdrawn from the shaker at pre-determined time intervals and the dye solution was separated from the adsorbent by centrifugation at 10,000 rpm for 20 min. The absorbance of supernatant solution was measured.

The effect of pH was studied by adjusting the pH of dye solutions using dilute HCl and NaOH solutions. The effect of adsorbent dosage was studied with different adsorbent doses (50–500 mg) and 50 ml of 50 mg L^{-1} dye at equilibrium time.

The amount of adsorption at time t and at equilibrium time and the percentage of dye removal were calculated by the following Eqs. (7) and (8).

$$q_t = [(C_0 - C_t)V]/W \qquad (7)$$

where C_0 and C_t (mg L^{-1}) are the liquid phase concentrations of dye at initial time and at any time t, respectively, V is the volume of the solution (L) and W is the mass of dry adsorbent used (g).

$$Removal\% = [(C_0 - C_e)/C_0] \times 100 \qquad (8)$$

where C_e is the equilibrium concentration of CR in solution (mg L^{-1}). All experiments were performed in duplicate and mean values are presented and taken for calculation purposes.

2.5. Desorption studies

After adsorption experiments, the CR loaded SHBG was separated out by filtration using Whatman filter paper No. 42 and the filtrate was discarded. The CR loaded SHBG was given a gentle wash with double-distilled water to remove the non-adsorbed CR if present. The dye loaded samples were agitated with distilled water by adjusting the initial pH from 2 to 12 for 180 min. The desorbed CR in the solution was separated by centrifugation and analyzed as before. The percentage of desorption was calculated.

2.6. FTIR analysis

FTIR spectra of pristine SHBG biomass are obtained by Thermo Nicolet, Nexus 670 Spectrometer with resolution 4 cm^{-1}.
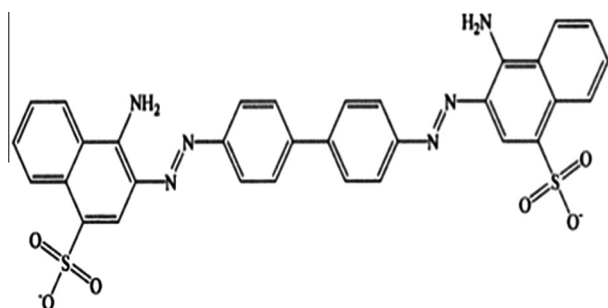
Pressed pellets were prepared by grinding the powder specimens with IR grade KBr in an agate mortar.

2.7. Scanning electron microscopy

Scanning electron microscopy of SHBG before and after adsorption is visualized by using Hitachi S-3000 N Scanning Electron Microscope (SEM).

2.8. Physical properties and surface area

Physical properties like apparent density and tap density were determined by using the method explained in Sinha, 1997. The procedures given in ASTM D 2015-72 procedure, 1979 were used for the determination of specific gravity, moisture and ash. The methods explained in the research paper of Rengraj, et al., 2002 were used for the determination of water soluble and acid soluble. pH and conductance of the extract of SHBG were measured by using the procedure described in ASTM D 1512-60 Procedure, 1960 and in the research paper of Wilde et al., 1972, respectively. Surface area of SHBG was determined by BET surface area method.

3. Results and discussion

3.1. Effect of SHBG dose

The effect of adsorbent (SHBG) dose on the removal of CR from the aqueous solution is shown in Fig. 2. The figure reveals that the removal of CR increases up to a certain limit (300 mg) and then it remains almost constant. An increase in adsorption with adsorbent dose can be attributed to increased surface area and the availability of more adsorption sites (Hameed, 2010). But the amount adsorbed per unit mass of the adsorbent decreases considerably. The decrease in unit adsorption with increasing dose of adsorbent is basically due to the adsorption sites remaining unsaturated during the adsorption process (Patil and Shrivastava, 2010). For the quantitative removal of CR, a maximum dose of 300 mg of adsorbent is required.

3.2. Effect of pH

Fig. 3 shows the effect of pH on the removal of CR by SHBG. When initial pH of the dye solution is increased from 5.85 to 11.02, the percentage removal decreased from 62.94 to 28.97. The lower pH Congo red solutions were not taken for the studies because at lower pH the solution turns to a black colour due to formation of quinoniod structure (Somasekhara Reddy, 2006). It is evident that the maximum removal of dye absorbed is at pH 5.85 and below. Low pH leads to an increase in H^+ ion concentration in the system and the surface of the SHBG acquires a positive charge by adsorbing H^+ ions. As the SHBG surface is positively charged at low pH, a significantly strong electrostatic attraction appears between the positively charged sites. A negatively charged surface site on the SHBG does not favour the adsorption of anionic CR molecule due to the electrostatic repulsion. Further, lower adsorption of the CR in alkaline medium is also due to the competition between excess OH^- ions and the anionic CR dye molecule for

the adsorption sites. A similar result is observed for the adsorption of CR on cashew nut shell (Senthilkumar et al., 2010), sun flower seed hull (Thinakaran et al., 2008), biogas waste slurry (Namasivayam and Yamuna, 1992), soy meal hull (Arami et al., 2006) and baggese fly ash (Mall et al., 2005).

pH of the CR solution was measured after adsorption and for clear understanding it is taken as final pH in the presence of CR. In a similar way, pH of the solution was measured after desorption and it is taken as final pH in the absence of CR. Initial pH of CR solution was plotted against final pH of solution in the presence and absence of CR and this plot is shown in
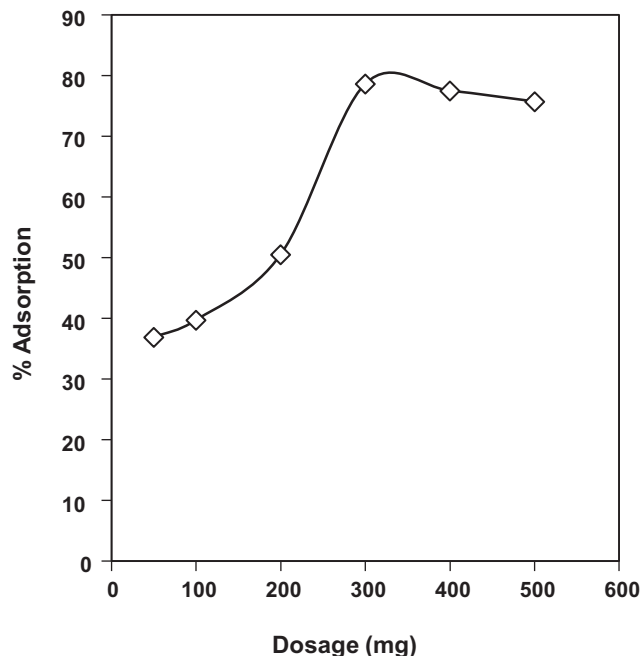

Figure 2 Effect of adsorbent dose on the adsorption of CR onto SHBG. Conditions: agitation time = 3 h; C_0 = 50 mg L^{-1}; V = 0.05 L; temp. = 30 ± 1 °C; speed of agitation = 160 rpm; pH 7.29; size of SHBG = > 53 < 75 μm.
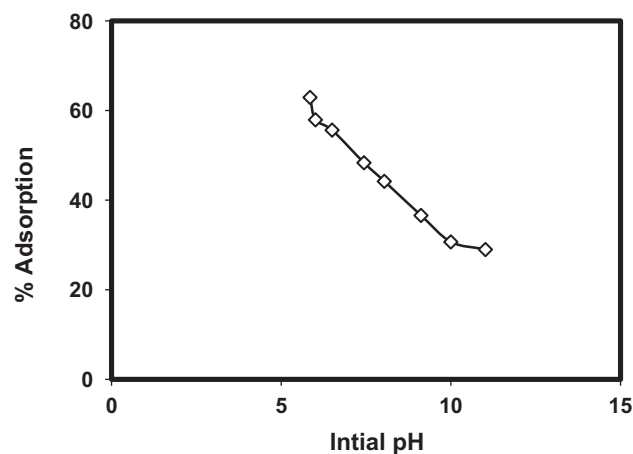

Figure 3 Effect of pH on equilibrium uptake of CR. Conditions as in Fig. 2 except pH.

Fig. 4. The results reveal that the final pH of Congo red solution after adsorption and after desorption is almost the same.

3.3. Kinetic study

3.3.1. Effect of initial dye concentration and contact time

The adsorption of CR on SHBG was studied at different CR concentrations (25–100 mg L^{-1}). Fig. 5 shows the result of the effect of initial concentration on adsorption of CR onto SHBG at 30 ± 1 °C. It is observed that dye uptake is rapid for the first 60 min and thereafter proceeds at a slower rate and finally attains saturation. Fig. 5 shows that an increase in the initial CR concentration results in increase in the adsorption of CR on SHBG. The equilibrium adsorption increases from 3.7915 to 20.0463 mg g^{-1}, with an increase in the initial CR concentration from 25 to 100 mg L^{-1}. Thus equilibrium removal of CR gets decreased from 89% to 74%. The dye attains equilibrium approximately at 1, 1.5, 2 and 2.5 h for dye concentrations 25, 50, 75 and 100 mg L^{-1}, respectively. However, the experimental data are measured at 180 min to make sure that a complete equilibrium is attained. It is clear that the removal of CR depends on the concentration 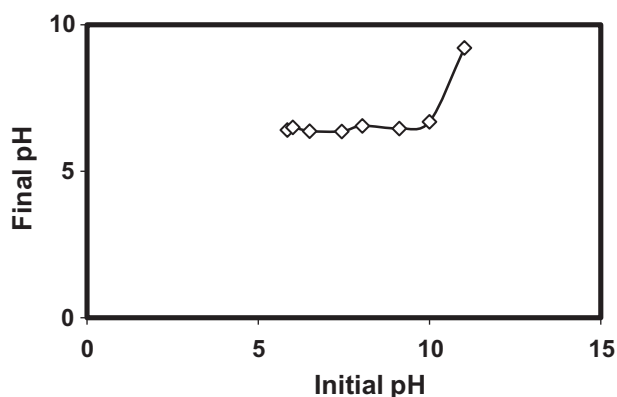of the dye. The removal curves are single, smooth and continuous leading to saturation. Hu et al. (2010), Somasekhara Reddy et al. (2012), Somasekhara Reddy (2006) studied and reported that the adsorption equilibrium of CR for cattail root, jujube seeds and tamarind fruit shell took 3, 3 and 7 h, respectively.

3.3.1.1. Adsorption kinetics.
For evaluating the adsorption kinetics of CR, the pseudo-first-order and pseudo-second-order kinetic models are used to fit the experimental data. Using Eqs. (1) and (2), $\log(q_e - q_t)$ versus t is plotted at different CR concentrations (Fig. 6). The pseudo-first-order model data do not fall on straight lines for most of the initial concentrations indicating that this model is less appropriate. The Lagergren first-order rate constant (k_1) is calculated from the model and is presented in Table 1 beside the corresponding correlation coefficients. The experimental kinetic data are further analyzed using the pseudo-second-order model. By plotting t/q_t against t for different initial CR concentrations (Fig. 7), a straight line is obtained in all cases and using Eq. (2), the second order rate constant (k_2) and q_e values are determined from the plots. The values of correlation coefficient are very high (R^2 are in between 0.989 and 0.9991) and the theoretical q_e cal values obtained, from this model are closer to the experimental q_e exp values at different initial CR concentrations (Table 1). It is important to note that for the pseudo-first-order model, the correlation coefficient obtained in this study, R^2 is in between 0.8878 and 0.9865, at different initial CR concentrations, is lower compared to the correlation coefficient obtained from the pseudo-second order model. Moreover, from Table 1, it is seen that the experimental values of q_e exp are not in good agreement with theoretical values calculated (q_e cal) from the pseudo-first-order equation. Therefore, it is concluded that the pseudo-second-order kinetic model provides a better correlation for the adsorption of CR on SHBG at different initial CR concentrations compared to the pseudo-first-order model. A similar result is reported for the adsorption of CR on jujube seeds (Somasekhara Reddy et al., 2012), methylene blue on jackfruit peel (Hameed, 2009) and on guava leaf powder (Ponnusami et al., 2008). The pseudo-first-order and pseudo-second-order kinetic models do not identify the diffusion mechanism. Thus the kinetic results are then analyzed by using the intra-particle diffusion model. Weber
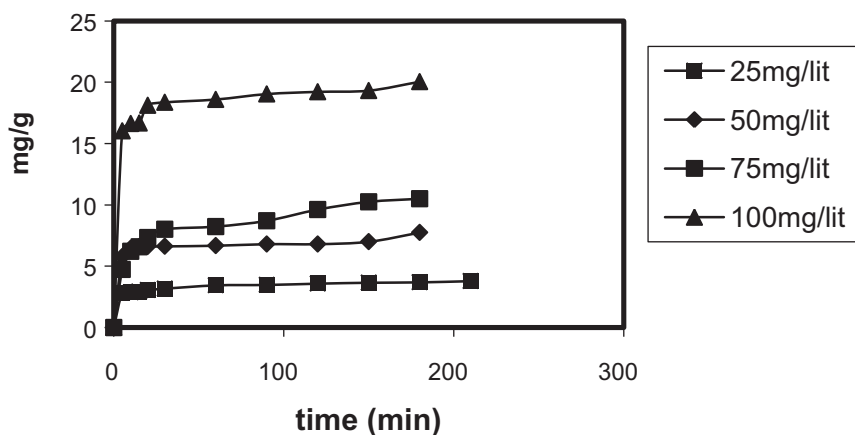

Figure 4 Initial pH vs. final pH of CR. Conditions as in Fig. 2.

Figure 5 Effect of initial concentration and contact time on CR adsorption. Conditions: V = 0.025 L; temp. = 30 ± 1 °C; speed of agitation = 160 rpm; size of SHBG = > 53 < 75 μm; dose = 100 mg; pH 7.29.
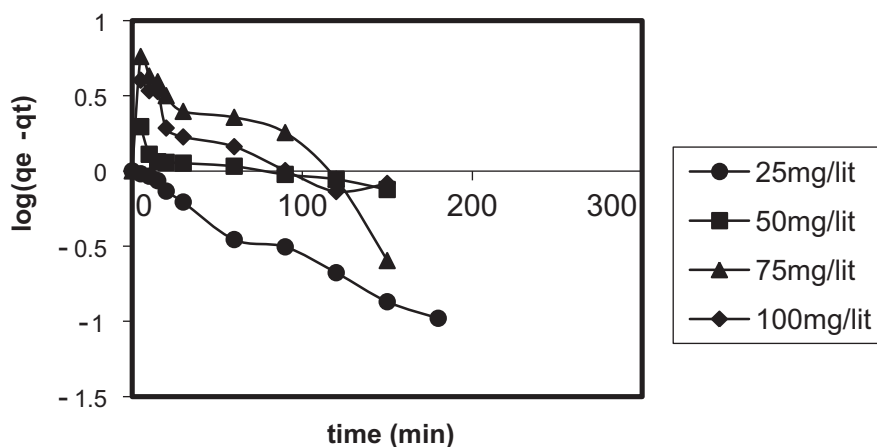
Figure 6   Lagergren pseudo-first-order plot.

Table 1   Pseudo-first-order and pseudo-second-order rate constants at 30 °C and different initial CR concentrations. Conditions: Size of SHBG = >53 < 75 m; pH of CR soln. = 7.29; Dose of SHBG = 100 mg; Speed of agitation = 160 rpm.

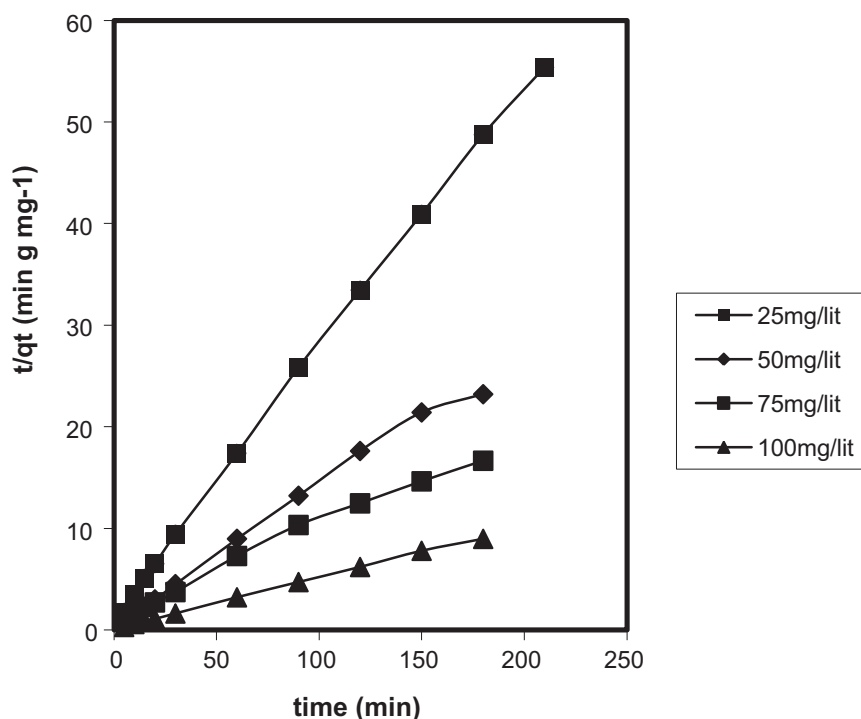| C_0 (mg L^{-1})	$q_{e\,exp}$ (mg g^{-1})	Pseudo-first-order model			Pseudo-second-order model		
		k_1 (min^{-1})	$q_{e\,cal}$ (mg g^{-1})	R^2	K_2 (g mg^{-1} min^{-1})	$q_{e\,cal}$ (mg g^{-1})	R^2
25	3.7915	0.012897	4.0622	0.9865	0.0658	3.8625	0.9988
50	7.7533	0.01515	8.2960	0.8898	0.03644	7.9029	0.9936
75	10.4989	0.017273	10.9895	0.9111	0.01001	11.0273	0.989
100	20.0463	0.013818	20.8641	0.8878	0.02353	20.2797	0.9991

Figure 7   Ho's pseudo-second-order plot.

and Moris model (Hameed and El-Khaiary, 2008a,b) is used with Eq. (3) to investigate intra-particle diffusion mechanism by plotting a graph between, q_t versus $t^{0.5}$ (figure is not shown).

If the intra-particle diffusion is the only rate-controlled step, then the plot shall pass through the origin. Else it is understood that the boundary layer diffusion controls the adsorption to

some degree (Hameed and El-Khaiary, 2008a). As seen from the plot q_t against $t^{0.5}$ the plots are not linear over the entire time range, implying that more than one process affected the adsorption and a similar behaviour is reported by (Hameed and El-Khaiary, 2008a). Further, the plot q_t versus $t^{0.5}$ shows at least two regions that represent boundary layer diffusion, and are followed by intra-particle diffusion in macro, meso, and micro pores (Hameed and El-Khaiary, 2008a). These two regions are
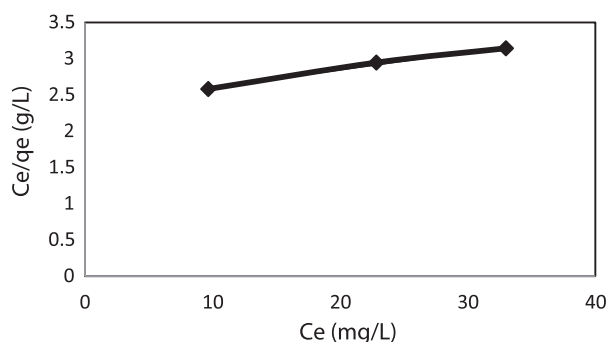

Figure 8 Langmuir isotherm plot for adsorption of CR onto SHBG.
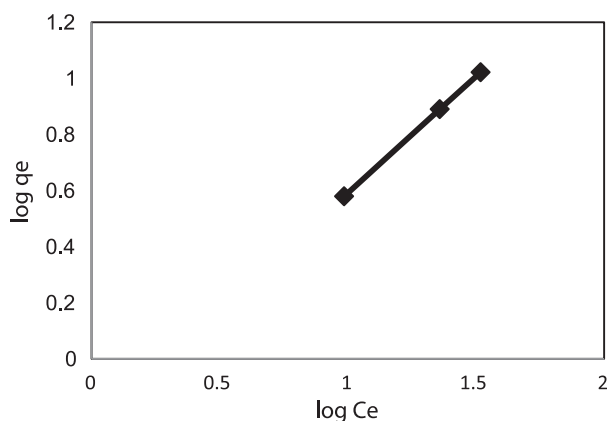

Figure 9 Freundlich isotherm plot for adsorption of CR onto SHBG.

followed by a horizontal line representing the equilibrium of the system. From q_t versus $t^{0.5}$ plot, two linear regions are observed. One at the beginning of adsorption, representing the rapid surface loading, followed by the second representing pore diffusion. The Microsoft Excel 2003 software package is used to analyze various regions and results of linear regression are obtained from the plot q_t versus $t^{0.5}$ for various initial concentrations. Intra-particle diffusion parameter, k_{pi}, is determined from the slope of each region, while the intercept of each region is proportional to the boundary-layer thickness. The calculated values of k_{pi} and the intercept, C, for all the linear regions are shown in Table 2.

3.4. Equilibrium modelling

Several mathematical models may be used to describe the experimental data of adsorption isotherms. In this study, the equilibrium data at different concentrations of CR and the adsorption of CR on SHBG are modelled with the Langmuir and Freundlich isotherm models. The details of the Langmuir and Freundlich isotherms are given in Eqs. (4)–(6). Langmuir adsorption isotherm plot is made between C_e and C_e/q_e and shown in Fig. 8. The Langmuir adsorption isotherm parameters, Q_{max} and K_L are calculated from the slope and intercept of the graph shown in Fig. 8. Freundlich adsorption isotherm plot is made between $\log C_e$ and $\log q_e$ and shown in Fig. 9. The Freundlich adsorption isotherm parameters, n and K_F are calculated from the slope and intercept of the graph shown in Fig. 9. The values of the parameters Langmuir and Freundlich obtained in these studies are presented in Table 3. The Langmuir and Freundlich isotherm models are well suited for the experimental data of CR on SHBG as per the coefficients of correlation.

The RL value for the adsorption of CR on SHBG is in between 0.4950 and 0.7968 as per Eq. (5), indicating that the adsorption is a favourable process.

3.4.1. Comparison of various low-cost adsorbents

The adsorption capacity of SHBG for the removal of CR is shown in Table 4. The adsorption capacity of various adsorbents for removal of CR is also shown in Table 4 for comparison and the removal capacity of SHBG is extremely good. Therefore, SHBG is considered to be an excellent adsorbent for the removal of CR from aqueous solution.

Table 2 Intra-particle diffusion constants for different initial CR concentrations at 30°C. Conditions as in Table 1.

Linear portion↓	Constants↓	$C_0 = 25$ mg/L	$C_0 = 50$ mg/L	$C_0 = 75$ mg/L	$C_0 = 100$ mg/L
First	K_{P1} (mg g^{-1} min$^{-0.5}$)	0.096	0.921	0.986	0.402
	C_1 (mg g^{-1})	2.594	1.134	2.783	15.2
	R^2	0.861	0.842	0.965	0.855
Second	K_{P2} (mg g^{-1} min$^{-0.5}$)	0.117	0.042	0.168	0.187
	C_2 (mg g^{-1})	2.533	6.407	7.037	17.24
	R^2	0.999	0.888	0.918	0.938
Third	K_{P3} (mg g^{-1} min$^{-0.5}$)	0.047	–	0.465	–
	C_3 (mg g^{-1})	3.063	–	4.406	–
	R^2	0.963	–	0.963	–

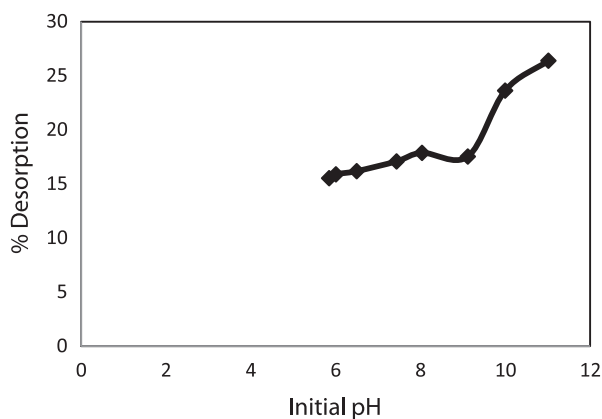**Table 3** Isothermal parameter values for the removal of CR on SHBG at different concentrations of CR solution.

Langmuir constants			Freundlich constants		
Q_{max} (mg g^{-1})	K_L (L mg^{-1})	R^2	K_F (mg g^{-1}) (L mg^{-1})$^{1/n}$	n	R^2
41.66	0.0102	0.99	0.5767	1.2048	1

Table 4 Adsorption capacities of CR on various adsorbents.

| S. no.	Name of adsorbent	q_e (mg g^{-1})	Reference
1	SHBG	41.66	Present study
2	Indian Jujube Seed	55.56	Somasekhara Reddy et al. (2012)
3	Jute stick powder	35.70	Panda et al. (2009)
4	Sunflower stalks	31.5–37	Hameed et al. (2008)
5	Cattail root	38.79	Hu et al. (2010)
6	Wheat bran	22.73	Wang and Chen (2009)
7	Rice bran	14.63	Wang and Chen (2009)
8	Tamarind fruit shell	10.48	Somasekhara Reddy (2006)
9	Alternanthera bettzichiiana plant powder	14.67	Patil and Shrivastava (2010)
10	Banana peel	11.2	Namasivayam et al. (1996)
11	Orange peel	7.9	Namasivayam et al. (1996)
12	Coir pith	6.72	Namasivayam and Kadirvelu (1994)
13	Banana pith	5.92	Namasivayam and Kadirvelu (1994)
14	Cashew nut shell	5.18	Senthilkumar et al. (2010)

3.5. Desorption

Desorption studies help to elucidate the mechanism of adsorption and recovery of the adsorbate and adsorbent. Regeneration of adsorbent makes the treatment process economical. The trend in the desorption process at different pH values is just converse to that of the adsorption process in the pH effect. This is shown in Fig. 10. The percent desorption is increased from 15.5 to 26.4 with an increase in pH from 6 to 11. This indicates that the desorption process is totally opposite to the adsorption process and CR adsorption is mainly due to ion exchange and physical adsorption (Asfour et al., 1985a). Similar type of observation is made in case of desorption of CR from the surface of jujube seeds (Somasekhara Reddy et al., 2012) and desorption of rhodamine-B from the surface of coir pith (Namasivayam et al., 2001).

3.6. Point zero charge

It is observed from Fig. 11 that the surface charge of the SHBG around pH 5.6 is zero. Hence, the pH_{PZC} at point of zero charge of the SHBG is 5.6. The effect of pH on the biosorption efficiency of CR is shown in Fig. 3. CR uptake is higher at lower pH. The high uptake of CR under acidic conditions is probably due to excessive positive charge on dye anion CR for the adsorption sites. As pH is increased above the pH_{PZC} value, which is found to be greater than 5.6, the adsorbent surface becomes predominantly negatively charged, enhancing the electro static repulsion between surface and CR anions. A similar behaviour is reported by the adsorption of CR on jujube seeds (Somasekhara Reddy et al., 2012), adsorption of reactive orange 16 on non-activated brazilian-pine fruit shell (Calvete et al., 2010) and adsorption of CR on biogas residual slurry (Namasivayam and Yamuna, 1995).

Figure 10 Desorption studies for the removal of CR by SHBG.
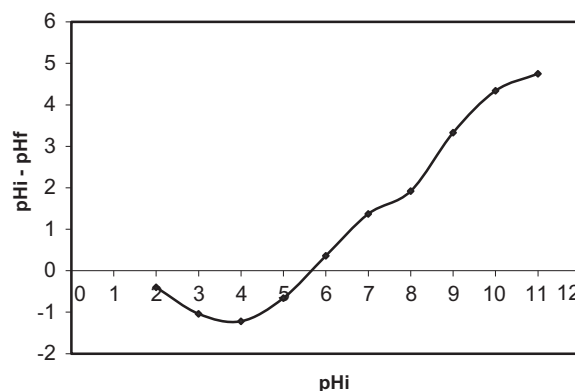
Figure 11 Determination of the point of zero charge of SHBG.

3.7. Cost analysis of SHBG waste adsorbent

Maximum adsorption capacity value was used to assess the quantity of adsorbent required to remove 1 kg of CR. This quantity was used as the basis for costing the adsorption process. The relative cost of adsorbents is shown in Table 5, together with adsorption cost to remove 1 kg of CR. Activated carbon was taken as a reference (Purkait et al., 2007) under almost all identical conditions of this study, having a comparative cost of unity. The results given in Table 5 indicate that the adsorption capacity of SHBG is 13.89% of that of activated carbon. The relative cost of the removal of CR by SHBG is only 4.1% of that of activated carbon. In addition, based on the low cost of the SHBG compared to activated carbon, there is no need to recover the SHBG and the exhausted SHBG can also be used as a fuel. Similar type of cost analysis was done by comparing the anionic dye, CR removal capacity of jujube seeds (Somasekhara Reddy

Figure 12 FTIR spectra of (a) SHBG alone and (b) CR loaded SHBG.

et al., 2012) and the anionic dye, astrazone blue removal capacity of hardwood with activated carbon (Asfour et al., 1985b). Relative costs of astrazone blue (anionic dye), maxilon red (anionic dye) and telon blue (cationic dye) removal by using number of low-cost materials like bagasse pith, maize cob and natural clay were also reported (Nassar and El-Geundi, 1991) based on the adsorption capacity of carbon. The cost estimation of another agricultural waste, coconut bunch for the removal of methylene blue was also reported (Hameed et al., 2008). These results indicate that the removal capacity of CR by activated carbon is higher than that of SHBG. However, an economic model indicated that SHBG may be economically attractive for the removal of CR from aqueous solutions.

3.8. Characterization of SHBG

3.8.1. FTIR analysis

The FTIR spectrum of SHBG is shown in Fig. 12 for SHBG and CR loaded SHBG. This figure shows that some peaks are shifted or disappeared and some new peaks are also detected. The change observed in the spectrum indicates the possible involvement of the functional groups on the surface of the SHBG in adsorption process. FTIR data of SHBG adsorbent are shown in Table 6.

3.8.2. SEM micrographs

Figs. 13 and 14 show the SEM micrographs of SHBG sample before and after CR adsorption. It is clear from these figures that SHBG has a considerable number of heterogeneous layers of pores. Thus, there is a good possibility for CR to be adsorbed. The surface of CR loaded-SHBG, however, clearly shows that the surface of SHBG is covered with CR molecules and the same is observed in Fig. 14.
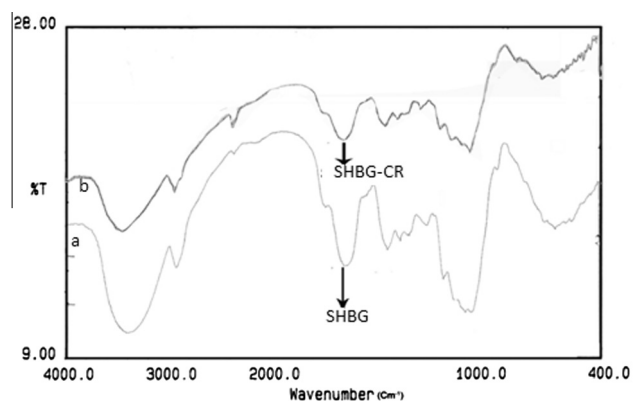
Table 5 Relative cost of CR removal.

Adsorbent	Adsorption capacity		Mass (kg) of adsorbent required to remove 1 kg of CR	Relative cost kg^{-1} adsorbent	Relative cost to remove 1 kg of CR	Reference
	mg g^{-1}	%				
Activated carbon	300	100	3.3333	1.000	1.000	Purkait et al. (2007)
SHBG	41.66	13.89	13.499	0.00759	0.041	Present study

Table 6 FTIR of SHBG adsorbent.

| IR peak	Frequency (cm^{-1})		Differences	Assignment
	Before adsorption	After adsorption		
1	3398.88	3435.53	−36.54	–OH stretch, H-bonded
2	2928.21	2922.42	5.79	–CH stretch (strong)
3	1736.09	1738.02	−1.93	–C=O stretch and stretch (strong) aldehyde
4	1643.50	1641.57	1.93	–C=O stetch (strong) amide
5	1433.24	1433.24	0	–
6	1369.58	1373.44	−3.86	N–H stretch (strong)
7	1327.14	1255.77	71.37	–C–H bending alkane
8	1240.34	1163.18	77.16	–C–F stretch (strong) alkyl halide
9	1161.25	1107.24	54.01	–
10	1103.38	1022.36	81.02	Associated with the C=O bond stretching of cellulose
11	1055.16	792.81	262.35	C–O stretch (strong)
12	1026.22	669.36	356.86	C–Cl stretch (strong)
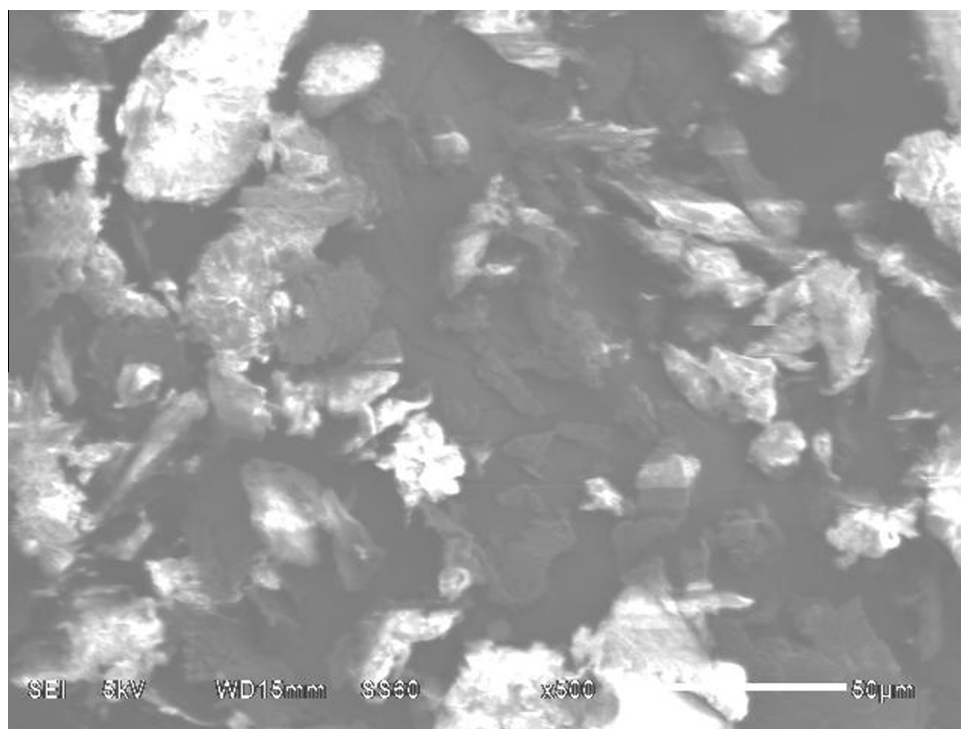
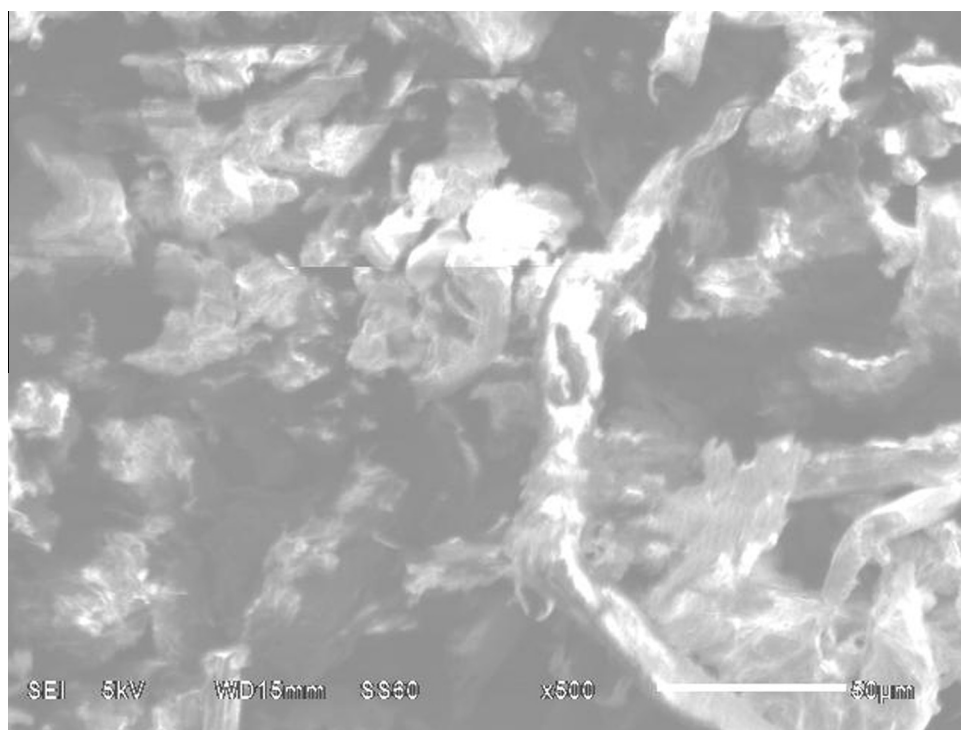**Figure 13**   Scanning electron microscopic photograph of SHBG.

Figure 14   Scanning electron microscopic photograph of CR loaded SHBG.

3.8.3. Physical properties and Surface area

The physical analysis of SHBG was done and the values are arranged in Table 7 along with the references from which analysis methods are adopted. The surface area of SHBG is also arranged in Table 7.

4. Conclusion

The present study establishes the fact that SHBG may be used as an adsorbent for the removal of CR from aqueous solutions. The amount of dye adsorbed is found to vary with initial

Table 7 Physical properties and surface area of SHBG.

Property	Size (μm)	SHBG	Reference
Apparent density (g/cm^3)	$> 53 < 75$	0.3420	Sinha, 1997
	$> 75 < 90$	0.3909	
	$> 90 < 150$	0.4813	
	> 150	0.5335	
Tap density (g/cm^3)	$> 53 < 75$	0.4943	
	$> 75 < 90$	0.5280	
	$> 90 < 150$	0.6104	
	> 150	0.6488	
Specific gravity	$> 53 < 75$	1.4093	ASTM D 2015-72 Procedure, 1979
	$> 75 < 90$	1.7887	
	$> 90 < 150$	1.8260	
	> 150	1.8940	
Moisture %	–	1.6039	
Ash %	–	1.2698	
Water soluble %	–	5.1650	Rengraj et al., 2002
Acid soluble %	–	0.3902	
pH	–	7.0860	ASTM D 1512-60 Procedure, 1960
Conductance (Micro Siemens/cm)	–	485	Wilde et al., 1972
BET surface area (m^2/g)	$> 53 < 75$	1.3636	
	$> 75 < 90$	1.0489	
	$> 90 < 150$	0.8950	
	> 150	0.7410	

CR concentration and contact time. The Langmuir adsorption isotherms are found to provide the best fit to the experimental data with a maximum adsorption capacity of 41.66 mg g^{-1}. The adsorption kinetics can be determined by pseudo-second-order kinetics. The results of the present investigation indicate that the SHBG has potential for use in removing CR from aqueous solutions.

References

Abbasi, M.N., Asl, R., 2008. Sonochemical degradation of Basic Blue 41 dye assisted by nanoTiO$_2$ and H$_2$O$_2$. J. Hazard. Mater. 153, 942–947.

American Society for Testing and Materials, 1960. ASTM D1512-60 Standard Methods for Testing Carbon Black, ASTM Philadelpia.

American Society for Testing and Materials, 1979. ASTM D143-52 Standard Methods for Testing Wood, Part 22. Standard Method for Testing Coal and Coke Part 26 ASTM D2015-72, ASTM Philadelpia.

Arami, M., Limaee, N.Y., Mohamoodi, N., Tabrizi, N., 2006. Equilibrium and kinetics studies for the adsorption of direct and acid dyes from aqueous solution by soy meal hull. J. Hazard. Mater. B 135, 171–179.

Asfour, H.M., Nassar, M.M., Fadali, D.A., Ei-Geundi, M.S., 1985a. Colour removal from textile effluents using hardwood saw dust as an adsorbent. J. Chem. Technol. Biotechnol. 35, 28–35.

Asfour, H.M., Fadali, O.A., Nassar, M.M., El-Geundi, M.S., 1985b. Equilibrium studies on adsorption of basic dyes on hardwood. J. Chem. Technol. Biotechnol. 35A, 21–27.

Asgher, Mahwish, Bhatti, Haq Nawaz, 2012. Evaluation of thermodynamics and effect of chemical treatments on sorption potential of Citrus waste biomass for removal of anionic dyes from aqueous solutions. Ecol. Eng. 38, 79–85.

Bhatnagar, A., Sillanppa, N., 2010. Utilization of agro-industirial and municipal waste materials as potential adsorbents for water treatment – a review. Chem. Eng. J. 157, 277–296.

Calvete, T., Lima, E.C., Cardoso, N.F., Vaghetti, J.C.P., Dias, S.L.P., Pavan, F.A., 2010. Application of carbon adsorbents prepared from Brazilian-pine fruit shell for the removal of reactive orange 16 from aqueous solution: Kinetic, equilibrium, and thermodynamic studies. J. Environ. Manag. 91, 1695–1706.

Carita, R., Marin-Morales, M.A., 2008. Induction of chromosome aberrations in the *Allium cepa* test system caused by the exposure of seeds to industrial effluents contaminated with azo dyes. Chemosphere 72, 722–725.

Celekli, A., Tanrıverdi, B., Bozkurt, H.S., 2012. Lentil Straw: a novel adsorbent for removing of hazardous dye – Sorption behaviour studies. Clean, Soil, Air, Water 00, 1–8.

Cheremisinoff, N.P., 2002. Handbook of water and wastewater treatment technologies. Butterworth-Heinemann, Boston.

Crini, G., 2006. Non-conventional low-cost adsorbents for dye removal: a review. Bioresour. Technol. 97, 1061–1085.

de Lima, R.O.A., Bazo, A.P., Salvadori, D.M.F., Rech, C.M., Oliveira, D.P., Umbuzeiro, G.A., 2007. Mutagenic and carcinogenic potential of a textile azo dye processing plant effluents that impact a drinking water source. Mutat. Res. 626, 53–60.

Demirbas, A., 2009. Agricultural based activated carbons for the removal of dyes from aqueous solutions: a review. J. Hazard. Mater. 167, 1–9.

Dogan, M., Abak, H., Alkan, M., 2008. Biosorption of methylene blue from aqueous solutions by hazelnut shells: equilibrium, parameters and isotherms. Water Air Soil Pollut. 192, 141–153.

Fan, L., Zhou, Y., Yang, W., Chen, G., Yang, F., 2008. Electrochemical degradation of aqueous solution of Amaranth azo dye on ACF under potentiostatic model. Dyes Pigments 76, 440–446.

Feng, Y., Yang, F., Wanga, Y., Maa, L., Wua, Y., Kerr, P.G., Yang, L., 2011. Basic dye adsorption onto an agro-based waste material – Sesame hull (*Sesamum indicum* L.). Biores. Tech. 102, 10280–10285.

Gong, R.M., Ding, Y., Li, M., Yang, C., Liu, H.J., Sun, Y.Z., 2005. Utilization of powdered peanut hull as biosorbent for removal of anionic dyes from aqueous solution. Dyes Pigments 64, 187–192.

Gupta, V.K., Suhas, I.A., 2009. Application of low-cost adsorbents for dye removal – a review. J. Environ. Manag. 90, 2313–2342.

Gupta, V.K., Mittal, A., Kurup, L., Mittal, J., 2006. Adsorption of a hazardous dye erythrosine over hen feathers. J. Colloid Interface Sci. 304, 52–57.

Gupta, V.K., Mittal, A., Jain, R., Mathur, M., Sikarwar, S., 2007a. Photochemical degradation of hazardous dye – safaranin-T using TiO2 catalyst. J. Colloid Interface Sci. 309, 460–465.

Gupta, V.K., Jain, R., Varshney, S., 2007b. Electrochemical removal of hazardous dye Reactofix Red 3 BFN from industrial effluents. J. Colloid Interface Sci. 312, 292–296.

Gupta, V.K., Mittal, A., Malviya, A., Mittal, J., 2009. Adsorption of carmoisine A from waste water using waste materials – bottom ash and de-oiled soya. J. Colloid Interface Sci. 355, 24–33.

Hai, F.I., Yamamoto, K., Fukushi, K., 2007. Hybrid treatment systems for dye wastewater. Crit. Rev. Env. Sci. Technol. 37, 315–377.

Hameed, B.H., 2009. Removal of cationic dye from aqueous solutions using jackfruit peel as non-conventional low-cost adsorbent. J. Hazard. Mater. 162, 344–350.

Hameed, B.H., 2010. Evaluation of papaya seed as a novel non-conventional low-cost adsorbent for removal of methylene blue. J. Hazard. Mater. 162, 939–994.

Hameed, B.H., El-Khaiary, M.I., 2008a. Removal of basic dye from aqueous medium using a novel agricultural waste material: pumpkin seed hull. J. Hazard. Mater. 155, 601–609.

Hameed, B.H., El-Khaiary, M.I., 2008b. Sorption kinetics and isotherm studies of a cationic dye using agricultural waste: broad bean peels. J. Hazard. Mater. 154, 639–648.

Hameed, B.H., Mahmoud, D.K., Ahmad, A.L., 2008. Equilibrium modeling and kinetic studies on the adsorption of basic dye by a low-cost adsorbent: coconut (Cocos nucifera) bunch waste. J. Hazard. Mater. 158, 65–72.

Hu, Z., Chen, H., Ji, F., Yuan, S., 2010. Removal of Congo red from aqueous solution by cattail root. J. Hazard. Mater. 173, 292–297.

Jaikumar, V., Shathish Kumar, K., Gnana Prakash, D., 2009. Biosoption of acid dyes using spent brewery grains: characterization and modeling. Int. J. Appl. Sci. Eng. 7, 115–125.

Kapdan, I.K., Ozturk, R., 2005. Effect of operating parameters on color and COD removal performance of SBR : sludge age and initial dyestuff concentration. J. Hazrd. Mater. B123, 217–222.

Khan, M.M.R., Ray, M., Guha, A.K., 2011. Mechanistic studies on the binding of Acid Yellow 99 on coir pith. Bioresour. Technol. 102, 2394–2399.

Kim, H.G., Park, C., Yang, J., Lee, B., Kim, S.S., Kim, S., 2007. Optimization of back flushing conditions for ceramic ultrafiltration membrane of disperse dye solutions. Desalination 202, 150–155.

Lorenc-Grabowska, E., Gryglewicz, G., 2007. Adsorption characteristics of Congo red on coal-based mesoporous activated carbon. Dyes Pigments 74, 34–40.

Mall, I.D., Srivastava, V.C., Agarawal, N.K., Mishra, I.M., 2005. Removal of Congo red from aqueous solution by bagasse fly ash and activated carbon: kinetic study and equilibrium isotherm analysis. Chemosphere 61, 492–501.

Namasivayam, C., Kadirvelu, K., 1994. Coir pith, an agricultural waste by-product, for the treatment of dyeing wastewater. Bioresour. Technol. 48, 79–81.

Namasivayam, C., Yamuna, R.T., 1992. Removal of congo red from aqueous solutions by biogas waste slurry. J. Chem. Technol. Biotechnol. 53, 153–157.

Namasivayam, C., Yamuna, R.T., 1995. Adsorption of direct red 12 B by biogas residual slurry: equilibrium and rate processes. Environ. Pollut. 89, 1–7.

Namasivayam, C., Muniasamy, N., Gayatri, K., Rani, M., Ranganathan, K., 1996. Removal of dyes from aqueous solutions by cellulosic waste orange peel. Bioresour. Technol. 57 (1996), 37–43.

Namasivayam, C., Radhika, R., Suba, S., 2001. Uptake of dyes by a promising locally available agricultural solid waste: coir pith. Waste Manag. 21, 381–387.

Nassar, M.M., El-Geundi, M.S., 1991. Comparative cost of colour removal from textile effluents using natural adsorbents. J. Chem. Technol. Biotechnol. 50, 257–264.

Neamtu, M., Yediler, A., Siminiceanu, I., Macoveanu, M., Kellrup, A., 2004. Decolorization of disperse red 354 azo dye in water by several oxidation processes – a comparative study 60, 61–68.

Oladoja, N.A., Aboluwoye, C.O., Oladineji, Y.B., 2008. Studies on castor seed shell as a sorbent in basic dye contaminated wastewater remediation. Desalination 227, 190–203.

Panda, G.G., Das, S.K., Guha, A.K., 2009. Jute stick powder as a potential biomass for the removal of Congo red and rhodamine B from their aqueous solution. J. Hazard. Mater. 164, 374–379.

Patil, A.K., Shrivastava, V.S., 2010. Alternanthera bettzichiana plant powder as low cost adsorbent for removal of Congo red from aqueous solution. Int. J. ChemTech Res. 2, 842–850.

Pavan, F.A., Lima, E.C., Dias, S.L.P., Mazzocato, A.C., 2008. Methylene blue biosorption from aqueous solutions by yellow passion fruit waste. J. Hazard. Mater. 150, 703–712.

Phalakornkule, C., Polgumhang, S., Tongdaung, W., Karakat, B., Nuyut, T., 2010. Electrocoagulation of blue reactive, red disperse and mixed dyes, and application in treating textile effluent. J. Environ. Manag. 91, 918–926.

Piccin, J.S., Gomes, C.S., Feris, L.A., Gutterres, M., 2012. Kinetics and isotherms of leather dye adsorption by tannery solid waste. Chem. Eng. J. 183, 30–38.

Ponnusami, V., Vikram, S., Srivastava, S.N., 2008. Guava, (*Psidium guajava*) leaf powder: novel adsorbent for removal of methylene blue from aqueous solutions. J. Hazard. Mater. 152, 276–286.

Purkait, M.K., Maiti, A., Das Gupta, S., De, S., 2007. Removal of Congo red using activated carbon and its regeneration. J. Hazard. Mater. 145, 287–295.

Raghavacharya, C., 1997. Colour removal from industrial effluents a comparative review of available technologies. Chem. Engg. World 32, 53–54.

Rengaraj, S., Moon, S.H., Sivabalon, R., Arabindoo, B., Murugesan, V., 2002. Agricultural solid waste for the removal of organics: adsorption of phenol from water and wastewater by palm seed coat activated coat. Waste Management 22, 543–548.

Santhi, T., Manonmani, S., 2011. Malachite green removal from aqueous solution by the peel of Cucumis sativa fruit. Clean, Soil, Air, Water 39, 162–170.

Senthilkumar, P., Ramalingam, S., Senthamarai, C., Niranjanaa, M., Vijayalakshmi, P., Sivanesan, S., 2010. Adsorption of dye from aqueous solution by Cashew nut shell: studies on equilibrium isotherm, kinetics and thermodynamics of interactions. Desalination 261, 52–60.

Sinha, A.K., 1997. Powder Metallurgy, Dhanpatrai Publishers (p) Ltd., New Delhi, pp. 33–37.

Slokar, Y.M., Le Marechal, A.M., 1997. Methods od decoloration of textile wastewaters. Dyes Pigments 37, 335–356.

Sohrabi, M.R., Ghavami, M., 2008. Photocatalytic degradation of Direct Red 23 dye using UV/TiO2: effect of operational parameters. J. Hazard. Mater. 153, 1235–1239.

Somasekhara Reddy, M.C., 2005. In: Utilization of agricultural wastes/by-products in treatment of water and wastewater, 2nd edition.. Wealth from Waste TERI Press, New Delhi, pp. 349-409.

Somasekhara Reddy, M.C., 2006. Removal of direct dye from aqueous solution with a novel adsorbent made from Tamarind Fruit Shell, an agricultural solid waste. J. Sci. Ind. Res. 65, 443–446.

Somasekhara Reddy, M.C., Sivarama Krishna, L., Varada Reddy, A., 2012. The use of an agricultural waste material, Jujuba seeds for the removal of anionic dye (Congo red) from aqueous medium. J. Haz. Mats. 203–204, 118–127.

Sonawane, G.H., Shrivastava, V.S., 2009. Kinetics of decolourization of malachite green from aqueous medium by maize cob (Zea maize): an agricultural solid waste. Desalination 247, 430–441.

Tanyildizi, M.S., 2011. Modeling of adsorption isotherms and kinetics of reactive dye from aqueous solution by peanut hull. Chem. Eng. J. 168, 1234–1240.

Thinakaran, N., Baskaraligam, P., Pulikesi, M., Panneerselvam, P., Sivanesan, S., 2008. Removal of acid violet 17 from aqueous solutions by adsorption onto activated carbon prepared from sunflower seed hull. J. Hazard. Mater. 151, 316–322.

Tsai, W.T., Hsien, K.J., Hsu, H.C., Lin, C.M., Lin, K.Y., Chiu, C.H., 2008. Utilization of ground eggshell waste as an adsorbent for the removal of dyes from aqueous solution. Bioresour. Technol. 99, 1623–1629.

Tsuboy, M.S., Angeli, J.P.F., Mantovani, M.S., Knasmuller, S., Umbuzeiro, G.A., Ribeiro, L.R., 2007. Genotoxic, mutagenic and cytotoxic effects of the commercial dye CI Disperse Blue 291 in the human hepatic cell line HepG2. Toxicol. In Vitro 21, 1650–1655.

Vieira, A.P., Santana, S.A.A., Bezerra, C.W.B., Silva, H.A.S., Chaves, J.A.P., Melo, J.C.P., Filho, E.C.S., Airoldi, C., 2011. Removal of textile dyes from aqueous solution by babassu coconut epicarp. Chem. Eng. J. 173, 334–340.

Vieira, S.S., Magriotis, Z.M., Santos, N.A.V., das Gracas Cardoso, M., Saczk, A.A., 2012. Macauba palm (Acrocomia aculeata) cake from biodiesel processing: An efficient and low cost substrate for the adsorption of dyes. Chem. Eng. J. 183, 152–161.

Wang, Xue.Song., Chen, Jing.Ping., 2009. Biosorption of Congo red from aqueous solution using wheat bran and rice bran: batch studies. Sep. Sci. Technol. 44, 1452–1466.

Wang, S., Li, H.T., 2007. Kinetic modeling and mechanism of dye adsorption on unburned carbon. Dyes Pigment 72, 308–314.

Wilde, S.A., Voigt, G.K., Iyer, J.G., 1972. Soil and Plant Analysis for Tree Culture, fourth edition. Oxford & IBH Publishing Co., New Delhi.

Wu, J.-S., Liu, C.-H., Chu, K.H., Suen, S.-Y., 2008. Removal of cationic dye methyl violet 2B from water by cation exchange membranes. J. Memb. Sci. 309, 239–245.

Zhang, W., Li, H., Kan, X., Dong, L., Yan, H., Jiang, Z., Yang, H., Li, A., Cheng, R., 2012. Adsorption of anionic dyes from aqueous solutions using chemically modified straw. Biores. Tech. 117, 40–47.